Since January 2020 Elsevier has created a COVID-19 resource centre with free information in English and Mandarin on the novel coronavirus COVID-19. The COVID-19 resource centre is hosted on Elsevier Connect, the company's public news and information website.

CHAPTER TWO

−1 Programmed Ribosomal Frameshifting as a Force-Dependent Process

Koen Visscher
Departments of Physics and Molecular & Cellular Biology, College of Optical Sciences, The University of Arizona, Tucson, Arizona, USA
E-mail address: visscher@email.arizona.edu

Contents

Abstract

−1 Programmed ribosomal frameshifting is a translational recoding event in which ribosomes slip backward along messenger RNA presumably due to increased tension disrupting the codon–anticodon interaction at the ribosome's coding site. Single-molecule physical methods and recent experiments characterizing the physical properties of mRNA's slippery sequence as well as the mechanical stability of downstream mRNA structure motifs that give rise to frameshifting are discussed. Progress in technology, experimental assays, and data analysis methods hold promise for accurate physical modeling and quantitative understanding of −1 programmed ribosomal frameshifting.

Progress in Molecular Biology and Translational Science, Volume 139
ISSN 1877-1173
http://dx.doi.org/10.1016/bs.pmbts.2015.11.003

1. –1 PROGRAMMED RIBOSOMAL FRAMESHIFTING

There is an increasing appreciation for the role of mechanical force in biological processes at the cellular and molecular scale both in vitro and in vivo.[1–5] A striking example that makes it easy to appreciate the role of mechanical force at the molecular level is the translation elongational cycle of the ribosome during protein synthesis, one of life's most fundamental processes. With peptidyl transfer RNA (tRNA) holding on to the growing peptide while residing in the ribosome's P site, aminoacyl transfer RNAs carrying amino acids in accordance with the codon sequence of messenger RNA enter and form a codon–anticodon pair in the aminoacyl or A site of the ribosome (accommodation). After a new peptide bond has formed, the P-site and A-site tRNA's are moved to the E (Exit) site and P site (translocation), respectively, threading paired mRNA through the ribosome. Translocation vacates the A site, allowing new tRNA to enter and bind (Fig. 1). The cycle repeats typically until a stop codon on the mRNA is reached. Since ribosomes can translate only single-stranded mRNA, complex mRNA structure motifs are unwound, by a mechanism that still remains obscure. Unlike initiation of translation for which several helicases have been identified[6] (eIF4A, DHX29, Ded1/DDX3, RHA/DHX9 to name a few), or where ribosomal protein S1 may be involved to unwind the mRNA[7] there are no known RNA helicases associated with the translocation of ribosomes along mRNA as part of the elongational cycle. How then do translocating ribosomes unwind the downstream mRNA structure they encounter? Work by Takyar et al. suggests that prokaryotic ribosomes have helicase activity themselves conferred on them by ribosomal proteins S3, S4, and S5, which encircle the mRNA entering the ribosome.[8] None of these

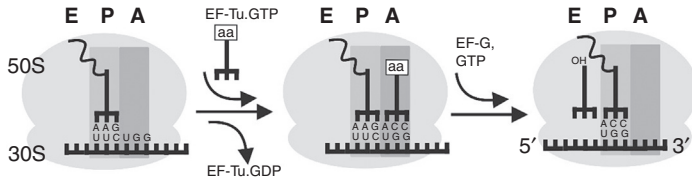

Figure 1 Simplified schematic of the translation elongational cycle. EF-Tu catalyzes the binding of tRNA in the A site, while EF-G catalyzes the translocation step, moving the tRNAs into the P and E sites. *Reprinted with permission from Skinner et al.*[15] *Copyright 2008 AIP Publishing LLC.*

proteins, however, have any ATPase activity that is usually associated with DNA and/or RNA helicases.[9] However, given the location of the helicase activity inside the mRNA tunnel, rotation of the 30S head relative to the 50S body could serve to shear the mRNA apart.[10,11] It is also in principle conceivable that ribosomes may simply be strong enough, building up sufficient tension when translocating the tRNA and associated mRNA, to unfold any downstream mRNA as it forces it into the narrow mRNA entrance tunnel. However, prokaryotic ribosomes stall out at a relatively low opposing force of approximately 13 pN (for comparison, *Escherichia coli* RNA polymerase can move against forces up to ~24 pN[12]), which seems to rule out any brute-force mechanisms for mRNA unfolding.[13] A recent single-molecule experiment indicates that ribosome helicase action during the translational elongation cycle may be twofold: it destabilizes the helical junction at the mRNA entry site favoring an open conformation, and it appears to pull mRNA strands apart during the translocation step when relatively large structural rearrangements occur on the ribosome.[14] Mechanical force may in principle assist in either activity.

When ribosomes translocate, tRNA and mRNA tension may build up in the single-stranded mRNA connecting the coding site (A and P sites) and any downstream mRNA structure not yet unwound that is being pulled against the mRNA entry tunnel. In response to such increased tension ribosomes may pause or stall; they may unwind the downstream structure; the codon–anticodon interactions at the A and P sites may be disrupted; or a combination of these events may occur. Such a prominent role of mechanical force has appeal for quantitative physical modeling of −1 programmed ribosomal frameshifting (−1 PRF). −1 PRF is a translational recoding event in which ribosomes slip backward, out of the reading frame by a single base in response to two *cis*-acting mRNA elements, a so-called slippery sequence at the ribosome coding site, and a downstream mRNA structure motif (pseudoknot, hairpin) at the entrance to the ribosome (Fig. 2).[16–18] Failure to unwind such a structure increases tension lowering the kinetic barrier for disruption of the codon–anticodon pairs at the slippery site.[19–21] The subsequent mRNA backward slippage, by a single nucleotide, is thought to relieve the tension so that the codon–anticodon interaction is reestablished but now in a −1 shifted reading frame. −1 PRF expands the information capacity of mRNA and is essential for the replication of (retro) viruses with minimal, compact genomes (eg, HIV-1, SARS). In many such systems, −1 PRF induces skipping of the 0-frame stop codon, giving rise to a fusion of structural and enzymatic proteins (to be further edited

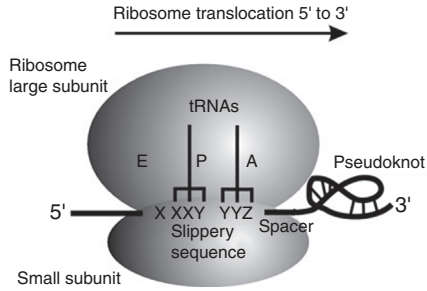

Figure 2 −1 Programmed ribosomal frameshift elements: slippery sequence at the coding site, spacer, and downstream RNA pseudoknot. *Reprinted with permission from Bailey et al.*[24] *Copyright 2014 IOP.*

posttranslationally). In a mechanical picture of −1 PRF, the probability of a frameshift, also known as the frameshift efficiency is determined by the stability of the codon–anticodon interaction at the slippery sequence,[22] the structural integrity of the downstream mRNA structure,[23] and the elastic properties of the spacer bridging both those elements.

When precisely in the translation elongational cycle the −1 frameshift occurs is still up for debate. Plant et al. have hypothesized that even tiny movements as small as 9 Å, thought to occur during the accommodation of tRNA, may increase tension and suffices to disrupt the codon–anticodon pairing when at the slippery sequence.[19] Recent theoretical modeling of −1 PRF shows that the 9 Å hypothesis is physically feasible, showing sharply peaked frameshift efficiencies only when ribosomes are at the slippery site.[24]

While this review addresses how force may be used to characterize elements in translation important for −1 PRF, it is worth pointing out that regulation of translation by force is not exclusively via mRNA, but may also act via other elements, for example, the emerging peptide. Goldman et al., recently demonstrated that mechanical force rescues stalled translation as part of the Sec protein-translocation pathway.[25] This pathway arrests translation as ribosome-nascent peptide chains are targeted to the membrane, that is, to the SecYEG transport channel.[26] Subsequently, the ATPase SecA is thought to physically pull on the nascent peptide restarting translation elongation and driving the peptide though the channel. An elegant single-molecule experiment by Goldman et al. demonstrated that pulling on the peptide with a mechanical force applied by optical tweezers indeed proved sufficient to restart translation elongation in arrested ribosomes.[25]

We will review methods and experiments that apply force to the single molecules to determine the mechanical properties of codon–anticodon interaction at the slippery site, the stability of downstream mRNA structure motifs that give rise to −1 PRF, and elastic properties of the ssRNA elasticity bridging those elements.

2. APPLYING MECHANICAL FORCES TO INDIVIDUAL MOLECULES

While it is next to impossible to apply well-controlled forces to molecules in traditional solution-based biochemical assays,[27] single-molecule techniques such as optical tweezers,[28] magnetic tweezers,[29–31] and atomic force microscopy[32] (AFM)-based force spectroscopy[33] allow forces ranging from sub-pN to the nN range to be applied to individual molecules. Pioneering experiments have included probing the motility of individual motor proteins,[34,35] the stretching of DNA molecules,[36] and the unfolding of giant muscle protein titin,[33] to name a few. These early studies have inspired a wide range of ever more advanced experiments targeting questions about the mechanochemistry of motor proteins[37]; the elastic and structural properties of DNA,[38] RNA,[39] and proteins,[40] as well as the interaction of these molecules with each other or with other ligands (protein-chaperone,[41,42] RNA kissing loops[43,44]).

2.1 Optical Tweezers

In optical tweezers a sharply focused laser beam traps microscopic particles near its focus,[28,45] exerting an approximately linearly increasing force as particles are moved away from the equilibrium position.[46–48] In other words, the optical tweezers act as a microscopic 3-dimensional (3D) spring that may be characterized by 3 spring constant k_x, k_y, and k_z, which are proportional to the laser light intensity used to generate the optical tweezers. In most implementations of optical tweezers, k_x and k_y are similar if not identical, whereas k_z is approximately 3–5 times smaller.[47] A variety of methods, generally based upon the Brownian motion of the particle in a harmonic potential and/or upon the response of the particle due to a known (fluid dynamic) disturbance, have been developed to calibrate these spring constants with ever increasing precision and accuracy.[47,49] Once the spring constants have been determined, forces are computed from the measured

displacement of the particle from the center of the tweezers. Optical tweezers have been shown to be ideally suited for exerting and measuring forces in the pN (10^{-12} N) regime. For large displacements the linear force–distance relation is lost and the tweezers is no longer spring-like. In fact a small region of constant force is encountered, which has been taken advantage of for creating a so-called passive constant-force trap.[50] Optical tweezers are not capable of trapping the molecules directly, but rather trap silica or polystyrene microspheres ranging in size from a few hundred nanometers to several micrometers that have been attached to the molecule of interest. To stretch and unfold individual molecules, the structural element of interest (RNA, DNA, protein) usually is sandwiched between two DNA handles that are then attached to the microsphere(s) held with the optical tweezers (Fig. 3).[51,52] Commonly used geometries include a single-beam setup with one handle attached to a solid surface, such as a microscope cover glass, while the other handle is held with the optical tweezers. The molecule may subsequently be stretched by laterally or vertically moving the microscope cover glass using a piezo-driven microscope stage. As indicated in Fig. 3A, due to the specific geometry of this assay, upon lateral movement of the microscope stage the microsphere is pulled and displaced not only laterally but also axially, demanding knowledge of k_x, and k_z as well as measurement of the displacements Δx and Δz to compute the direction and magnitude of

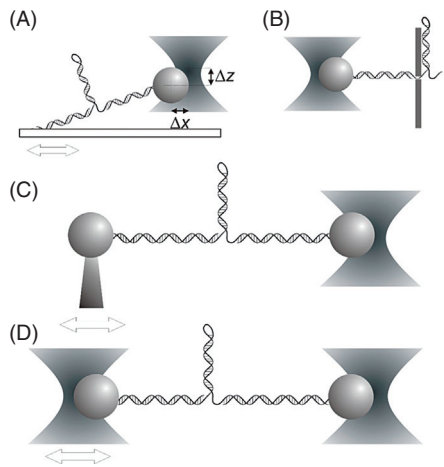

Figure 3 Optical tweezers geometries. (A) Surface tethering. Stage movement induces lateral as well as axial microsphere displacement in the optical tweezers. (B) Optical tweezers-nanopore arrangement. (C) Micropipette-optical tweezers arrangement. (D) Dumbbell arrangement (not to scale).

the force exerted in the direction along the molecule.[53] While initially in these assays the measurement of Δz proved problematic and k_z and Δz were estimated or computed indirectly,[53] it was later realized that the so-called back-focal plane position detection[54,55] provides a direct measurement of Δx, Δy, as well as of Δz with the latter being proportional to the total light intensity impinging on the photosensitive sensor.[56] Recent technological advances have taken advantage of this development and produced ultrastable (low drift) and extremely high precision and resolution optical tweezers specifically for use with the surface-attachment geometry.[57,58]

However, axial displacement in the optical tweezers may be eliminated altogether by avoiding any surface-coupling and alternatively attaching this handle to a microsphere held on a micropipette[51] as indicated in Fig. 3C. Upon proper alignment lateral displacement of the micropipette force measurement then only requires measurement of Δx for accurate computation of force. It is noted that in early implementation of this assay two counter-propagating, moderately focused laser beams were used to form a 3D trap; an arrangement that allows for direct measurement of force (by conservation of momentum).[59]

A preferred assay involves a dumbbell geometry in which the molecule is held in between two optical tweezers (Fig. 3D). This geometry in principle holds significant practical advantages over the other geometries. Instrumental drift is much reduced as the molecule, handles, and beads are suspended in a fluid and do not have any direct mechanical interaction, that is, contact with the instrument. Remaining drift due to laser beam pointing instabilities may be further reduced by traditional-type laser beam stabilization techniques utilizing feedback schemes and/or immersing essential optical paths in helium.[60] Such measures allow for subnanometer, Angstrom level resolution position measurements of trapped particles. In addition, when the positions of the microspheres in both traps are measured simultaneously, correlation analysis may provide further enhancement of the position signal to noise ratio.[61] While in principle not limited to this geometry, the dumbbell assay saw the first implementation of the so-called passive constant-force tweezers or force clamp.[50] Constant-force optical tweezers were pioneered to study the force dependence of the mechanochemistry of the kinesin motor protein.[37,48] This force clamp applied a (digital) feedback to assure a constant distance between the center of the tweezers and the microsphere, thus maintaining a constant force. It has been shown however that the limited time-response of the feedback loop may directly affect the kinetics of unfolding and refolding of molecules held near the transition

force.[62] A passive force clamp eliminates the need for any active feedback by pulling one of the microspheres in the dumbbell assay to a region of the optical tweezers where the potential is linear and thus the force is constant.[50] This region typically is small, ~50 nm, limiting its use to the unfolding of small molecules only. Recently by shaping the trapped particles Phillips et al. were able to increase the constant-force region to several microns.[63] It remains to be seen if the relatively large particles for which this was demonstrated prove practical and advantageous for single-molecule unfolding studies, but the idea is interesting as it could allow access to the unfolding of much larger molecules.

With the bandwidth and dead-time limitation of active feedback resolved, folding kinetics may subsequently be derived after correcting the remaining instrument response due to the tweezers' spring constant and compliance of the DNA handles.[64] Constant-force dumbbell assays may also be implemented using counter-propagating laser beams, which allow for shorter than usual DNA handles if so desired.[65,66]

While the emphasis of this review is on the use of optical tweezers for unfolding individual molecules alternative techniques deserve mentioning and in some cases be more beneficial for particular applications.

2.2 Magnetic Tweezers

Magnetic tweezers based assays appear similar to the surface-coupled geometry used with optical tweezers but now the molecule is stretched vertically between the surface and a magnetic bead (Fig. 4A).[30] Two magnets suspended above the bead provide a magnetic field gradient resulting in typical forces in the pN range, its magnitude set by the height of the magnets (or electrical current if electromagnets are used). The typical magnetic field gradient however is sufficiently shallow so that magnetic tweezers are by their nature a constant-force single-molecule technique. The force applied

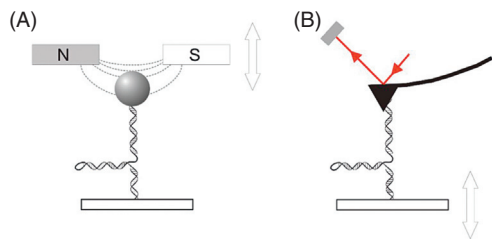

Figure 4 (A) Magnetic tweezers. (B) AFM-based force spectroscopy (not to scale).

remains constant over the dimensions of the molecule, that is, independent of its state, folded or unfolded. As the force is applied vertically, the particle's displacement upon unfolding is usually determined with nanometer resolution from the degree of defocus observed in the microscope using image processing. The axial spring constant, k_z is readily determined from lateral particle displacement fluctuations (Brownian motion) once realizing the system entails an inverted pendulum.[30] It is of interest that axial, vertical stretching is now also used on occasion with optical tweezers enabling the use of short tethers.[67]

While many single-molecule methods readily allow the observation of repeated unfolding and refolding of one particular molecule, sampling a large number of molecules remains time-consuming. However, magnetic tweezers are of particular interest because they hold promise for (massively) parallelization of single-molecule experiments: many surface-coupled beads may readily be observed within one field-of-view of the microscope[68] with all molecules potentially held at the same force. Such parallelization, although in principle not impossible with optical tweezers is more readily achieved using magnetic tweezers in which the magnetic field is applied over a large area that in principle could contain tens to hundreds of surface-tethered particles. It is also noted that recently centrifugation has been reintroduced to exert forces on individual molecules in a massively parallel fashion.[69] However, to date this method does not appear to have been widely adopted.

2.3 AFM

AFM has traditionally been applied for force spectroscopy of individual proteins or protein repeats, in particular the giant protein titin (Fig. 4B).[33] In AFM a cantilevered sharp tip probes the surface which the molecule of interest has been deposited on and/or attached to. As it moves along the surface, the tip approaches and retracts from the surface, detecting a tip-molecule attachment as the cantilever deflects upon retraction. This bending of the cantilever is determined by measuring the deflection of a laser beam reflected off the end of the cantilever using a position-sensitive photo detector. The spring constant of the cantilever is generally determined by analysis of its thermal fluctuations, in much the same way as the optical tweezers use Brownian motion. Other methods exist, for a review see Cumpson et al.[70] While typical cantilevers have spring constants far exceeding those of optical tweezers resulting in typical forces of order nN, softer

cantilevers have become available allowing forces in the pN regime to be measured or applied. Furthermore, recent technical improvements reducing drift and increasing tip-sample stability to as small as 100 pm have the potential of bringing AFM to single-molecule unfolding experiments that would otherwise employ optical tweezers.[71] Also note that such stability in principle makes previously impossible constant-force experiments feasible. AFM would then hold the advantage that it is more readily automated to scan the surface for viable candidates for stretching; unfold and refold the molecule a predetermined number of times; then break the tether and move on to the next. Since typically the tip-molecule attachment is nonspecific it is not always clear which part of the molecule is unfolded, or worse if the molecule or something else altogether has been stretched. One therefore tends to construct repeat sequences of the structures of interest which serve as a fingerprint of the molecule.[72] For example, in a five-repeat structure one may decide to only analyze data displaying three or more repeats, thus maximizing the probability that the desired molecule is being unfolded. However, since it was shown that unfolding forces depend upon the number of unfolded domains in a chain, so-called order statistics need to be applied for generating proper parent distribution functions[73] of unfolding forces before such data can further be utilized for analysis and/or predictions of kinetic behavior. While this analysis assumes repeats of identical noninteracting domains governed by a single underlying parent force distribution function, in principle the same applies when unfolding sequences of nonidentical structural domains, such as complex molecules[74] in which case the unfolding forces are pulled from multiple differing parent distributions. Successful statistical order correction may then depend on the ability to recognize which type of domain is unfolded (eg, by difference in change of extension) so as to assign the observed unfolding event to the proper associated parent distribution.

2.4 Nanopores

Biological (eg, α-hemolysin[75,76]) and man-made solid-state[77–79] nanopores enable mechanical unfolding of bare proteins and nucleic acids without the need for any handles or microspheres, thus potentially easing the interpretation of data and derived kinetics.[80] The molecules are forced through a nanometer scale hole due to an electrical potential applied across the pore interrupting the baseline electrical current as the molecule resides in the pore. Unfolding of structures initially too big to pass through and blocking

the current may be detected as a sudden increase in the current after they unfold and then zip through the pore. By ramping up the potential difference across the pore, a distribution of unfolding voltages can thus be acquired. Alternatively, one may choose to operate at constant voltage and record the time required for unfolding to occur. In many respects this is analogous to the use of optical tweezers with voltage taking the role of force. However, while nanopore-based experiments sample only a single unfolding event for each of the many molecules passing through sequentially, optical tweezers experiments do the opposite and are better suited to sample many repeated unfolding and refolding events for only one single molecule. Also, unlike optical tweezers the magnitude of the actual force applied remains largely unknown. Efforts have been made to measure this force directly using optical tweezers and nanopores in a combined setup (Fig. 3B).[81] Interestingly, in such an arrangement one could imagine using the optical tweezers to pull a molecule through the nanopore (in the absence of any electrical potential) potentially mimicking how ribosomes pull through and unravel structured mRNA. Although such type of experiments have been proposed[81,82] actual data remains scarce, if nonexistent. For a more extensive discussion see chapter: Studies of RNA Sequence and Structure Using Nanopores.

3. VARYING OR CONSTANT FORCE PROTOCOLS

Molecules may be unfolded following a variety of stretching protocols: one may, for example, slowly or quickly ramp up the force in a linear fashion (force ramp); apply a sudden change in force (force jump); or hold the system at a constant force at all times.[83]

3.1 Force-Ramp Mode

A force ramp is generated simply by moving one of the ends of molecular construct away from the opposing end, usually at a constant speed. As the construct is stretched the force increases accordingly and is determined by measuring the position of the microsphere in the optical trap or magnetic tweezers, or the deflection of the AFM tip. When the force ramp is shallow and the molecule is pulled slowly, that is, slower than the intrinsic kinetic (un)folding rates of the molecule, the (un)folding event occurs at or very near to thermodynamic equilibrium. Equilibrium behavior is readily recognized in recorded force-extension data: the sudden increase in extension upon

unfolding during stretching occurs at the same force as the drop in extension upon relaxation of the molecule.[51] In other words, the extension and relaxation curves overlap. At equilibrium conditions, equilibrium thermodynamic quantities such as the free-energy change of the reaction (ΔG) are readily derived once the elastic response of the DNA handles has been accounted for.[51,84,85] However, equilibrium conditions cannot always be met and are often limited to a relatively small group of molecules, such as short DNA and RNA stem loops that lack tertiary interaction and when structural properties are predominantly governed by Watson–Crick base pairing. Nevertheless, even with these molecules, experiments can quickly be driven away from equilibrium by stretching (and relaxing) the molecule more rapidly. In particular, tertiary interactions quickly drive experiments away from equilibrium so that unfolding and refolding forces differ significantly, even at moderate to low ramp rates (an example is shown in Fig. 6). In many cases equilibrium conditions simply prove impractical experimentally as low ramp rates put ever-increasing demands upon instrument stability and drift.

Departure from equilibrium is not as problematic as it may appear. So-called fluctuation relations, such as the Jarzynski's equality and Crooks' fluctuation theorem provide a theoretical framework for deriving equilibrium free energy differences from nonequilibrium work measurements.[86,87] Small RNA hairpins, whose (un)folding using optical tweezers could readily be tuned from near- to off equilibrium by adjusting the force-ramp rate, have successfully served to verify these methods.[88,89] However, applying fluctuation relation may put unexpected demands upon experimental procedures as demonstrated by Ribezzi-Crivellari et al. who point out that the work measurement then should ideally be based upon a force measurement in the moving, not in the static optical tweezers as is customary in dumbbell geometries.[66]

Nonequilibrium measurements also do not preclude the determination of the energy landscapes underlying the physics of molecular folding.[90] Therefore, in some cases it may in fact be advantageous to create off-equilibrium conditions, and to increase ramp rates to ensure low-drift, high-stability experimental conditions.

3.2 Constant-Force Mode

Repeated unfolding and (re)folding events can be recorded for systems at equilibrium by keeping the applied force constant at the characteristic (un)

folding force. In the data one would observe the extension to "hop" between two or more discrete mean values representing the folded, unfolded, and possibly intermediate states. For most such experiments, a dumbbell-type passive constant-force optical tweezers is preferred as it circumvents bandwidth issues apparent in active feedback system, and provides a stable, low-drift solution for maintaining a constant force.[50,62] Equilibrium experiments readily allow for the determination of folding energy landscapes. From such experiments, the folding energy landscape $U(x)$ in principle is readily obtained from the histogram or probability distribution of the molecule's extension, $P_{\mathrm{mol}}(x)$ as these quantities are related by the Boltzmann distribution at equilibrium[64,90]:

$$P_{\mathrm{mol}}(x) \propto e^{-U(x)/k_{\mathrm{B}}T}$$

However, the real experiment measures $P(x)$, a histogram of microsphere position which also includes contributions due to compliance of the trapped microspheres (the force probe) and the DNA handles, which can be written as a convolution of $P_{\mathrm{mol}}(x)$ and a response or point spread function PSF(x) characteristic of the assay used.

$$P(x) = \mathrm{PSF}(x) \otimes P_{\mathrm{mol}}(x),$$

The assay's PSF(x) can be determined by recording microsphere position histograms at identical conditions, but by using the DNA handles microsphere(s) construct without the folded structure motif present. $P_{\mathrm{mol}}(x)$ is subsequently computed by applying a (nonlinear) deconvolution algorithm, after which the 1D energy profile readily follows[90]:

$$U(x) \propto -k_{\mathrm{B}}T \ln P_{\mathrm{mol}}(x)$$

The constant-force method relies on the relatively rapid acquisition of a large amount of folding and unfolding events, thus ensuring that the energy barrier separating the folded and unfolded states, where the system spends the least of its time, is also sufficiently sampled. This requirement becomes increasingly hard to meet when the height of the barrier increases and the barrier top becomes rarely sampled by the molecule, leading to impractically long measurement times. To circumvent this problem, de Messieres et al. adopted an umbrella sampling style technique in which a stiff force probes (optical tweezers, AFM) harmonically constrain excursions along the reaction coordinate, but is stepped along the reaction coordinate.[67] As the probe is moved along the reaction coordinate, the otherwise (ie, in constant-force

mode) rarely sampled regions are effectively addressed, enabling rapid data acquisition. Landscapes thus reconstructed were in good agreement with those derived from constant-force measurements.

Alternatively one may apply force ramp or jump experiments to sample more closely near (high) energy barriers. However, while the reconstruction of the energy landscape $U(x)$ is rather intuitive at equilibrium conditions, more involved methods, either model independent or model dependent, must be applied to reconstruct energy landscape from nonequilibrium data. Applicability, limitations, advantages, and disadvantages of these approaches have been comprehensively addressed in a recent review by Woodside and Block, and will not be repeated.[90]

4. PROBING −1 PRF ELEMENTS WITH FORCE

4.1 Unfolding RNA Hairpins and Pseudoknots

To theoretically appreciate the effect of force upon mRNA unwinding or unfolding, it is insightful to think of folding as a minimum-energy search on the surface of a landscape reflecting the energetics of the molecular conformations.[91] Such analysis may assist in a quantitative understanding of −1 PRF as it would allow for comparing the thermodynamics and kinetics of the downstream mRNA unfolding with the dynamics and energetics of the disassociation and reassociation of the mRNA codon and tRNA anticodons at the associated slippery sequence. However, given the large number of degrees of freedom of even the smallest RNA molecules, these energy landscapes are highly multidimensional allowing, in principle, multiple pathways from an unfolded to the lowest-energy folded conformation. Experiments usually only resolve a 1D projection of the multidimensional landscape onto a single reaction coordinate (Fig. 5). For example, in the case of mechanical unfolding the end-to-end distance or extension of the molecule appears a natural choice for a reaction coordinate. However, can such a condensed 1D projection capture the relevant thermodynamics and kinetics of the systems studied? In other words, what makes a "good" reaction coordinate? This is an important question as a poor choice of reaction coordinate may quickly lead to incorrect interpretation of data and to wrong conclusions.[90,92] Recent work has started to address this question more rigorously. One may demand that a "good" reaction coordinate faithfully captures the folding kinetics observed in data and provides predictions on the

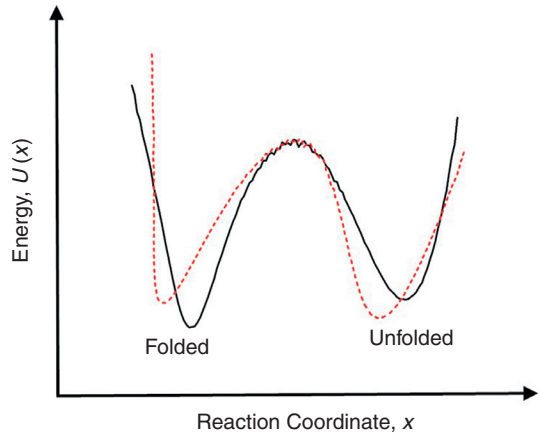

Figure 5 1D energy landscape with a kinetic barrier separating the unfolded and folded states. Application of force tilts the landscape [dashed (red dashed in the web version)] so as to lower the barrier from the folded state promoting escape to the unfolded state.

outcome of a pathway. But since the choice of reaction coordinate is typically not free but experimentally constrained, how can one test and confirm that the experimentally accessible reaction coordinate is in fact a "good" coordinate. Work by Du et al. introduces the split probability or committer, $p_F(x)$, as a reaction coordinate quality test.[93]

With reference to the energy landscape shown in Fig. 5, $p_F(x)$ is defined as the probability along the reaction coordinate x of reaching the folded state. Ideally, $p_F(x)$ should approach 0 when in the unfolded state, 1 in the folded state, and a ½ when at the top of the barrier separating the two energy minima, the latter condition then a reasonable minimum requirement for a "good" reaction coordinate. Upon such analysis by Chodera et al. the end-to-end distance appeared at first a poor reaction coordinate for unfolding DNA hairpins using optical tweezers.[94] However, subsequent work by Neupane et al., who carefully accounted for any effects of the extra fluctuations due to compliance of DNA handles and microspheres in the optical tweezers, did find the end-to-end distance to be a good reaction coordinate.[95] Rather than $p_F(x)$ however, they evaluated a related, perhaps more robust quantity, the conditional probability $p(x|\mathrm{TP})$ that the molecule is on a transition path when the end-to-end distance equals x, a function that sharply peaks near the top of the barrier where it should approach ½. One concludes that (un)folding of simple DNA hairpins near equilibrium can be considered a 1D diffusion problem.[95] While this analysis proved successful

for relatively simple molecular structures, it remains to be seen if the same conclusion will hold for more complex architectures containing tertiary interactions prevalent in proteins and many RNA molecules.[74,96] In any case, the analysis framework for testing reaction coordinate quality should be directly applicable to such systems. It may be fair to demand that single-molecule unfolding studies include a reaction coordinate quality test if any energy landscape and/or kinetics are to be derived from single-molecule unfolding data.

As previously discussed, it is not a stretch of the imagination to suppose a correlation between mRNA pseudoknot stability, measured as an unfolding force, and −1 PRF efficiency. However thus far, single-molecule studies of unfolding of −1 PRF-stimulating mRNA structures have predominantly focused on determining unfolding forces with little analyses in terms of energy landscapes and/or kinetics and with little to no attention to the "goodness" of the reaction coordinate. There currently appears somewhat of a disconnect between the advanced analysis methods that have proven successful for small, simple hairpin structures and the unfolding of more complex perhaps more biologically relevant structures.

Stepwise unfolding of large complex RNA structures may provide a fingerprint of its structure when it is dominated by secondary interactions, Watson–Crick base pairing and unfolding proves hierarchical.[74] However, for very short mRNA structures that are dominated by tertiary interactions such fingerprinting is likely to fail. For example, in the case of the Beet Western Yellow Virus RNA pseudoknot (Fig. 6) in which a quadruple base interaction of residue C8 is thought to sustain its compact structure, only the

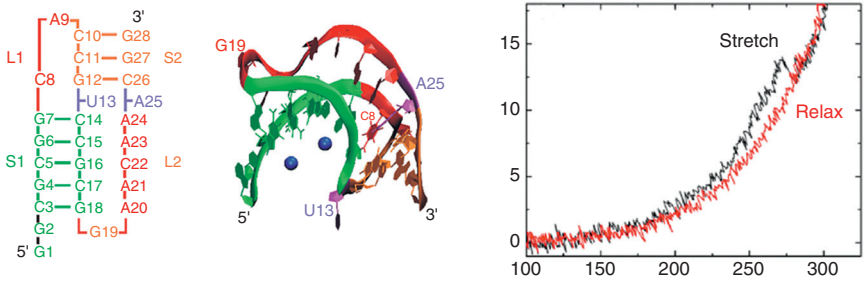

Figure 6 BWYV pseudoknot structures with the C8U substitution mutant's force-extension curves as obtained with surface-mounted optical tweezers in force-ramp mode. Unfolding occurs at a force of ~13 pN, whereas refolding is not observed upon relaxation. *Reprinted with permission from White et al.[97] Copyright 2011 American Chemical Society.*

unfolding of stem 1 could explicitly be identified by the increase in extension.[97] Moreover, upon changing pH and/or mutating residue C8 such correlations could no longer be established.

Thus it is not surprising that stretching studies of −1 PRF RNA pseudoknots have thus far focused on determining the forces required for unfolding wild-type and mutant structures that have increased or reduced frameshift efficiency. While early stretching studies indicate that a correlation between frameshift efficiencies and unfolding force exists,[98,99] later studies fail to establish any such correlation.[97,100,101] Interestingly, Ritchie et al. propose a correlation with conformational plasticity of the pseudoknot rather than with force, consistent with White's observation that BWYV mutant pseudoknots abolishing −1 PRF in fact yield slightly higher unfolding forces and may be accessing multiple unfolding pathways much unlike the wild-type BWYV pseudoknot.[97,101] Furthermore, −1 PRF-suppressing ligands also appear to inhibit such required structural plasticity in the SARS coronavirus pseudoknot.[102] A recent single-molecule analysis of the nonviral, human −1 PRF signal in CCR5 mRNA also has yielded multiple conformers and unfolding pathways.[103]

It is hard to judge how appropriate and insightful these unfolding experiments truly are for a quantitative physical understanding of −1 PRF. During the translational elongation cycle, the mRNA, rather than being stretched from both ends, is threaded through the narrow entry tunnel to the ribosome, leaving one end free. Therefore, both scenarios may access significantly different unfolding pathways on a multidimensional energy landscape. Such concern may suggest alternative experimental geometries in which individual RNA molecules are pulled through nanopores, ideally in a controlled fashion using optical tweezers to apply well-defined forces.[82]

Unfolding by optical tweezers, or as proposed using nanopores are, with "bare" mRNA molecules, that is, in the absence of any upstream ribosomes. It will be of interest to see if ribosome-positioned upstream significantly affect pseudoknot unfolding force, unfolding pathways, and plasticity.[104,105] Single-molecule assays that probe the codon–anticodon dynamics at the slippery sequence and investigate the force dependence of the translation elongational cycle (discussed later in the chapter; see Fig. 8) should be fit to answer these questions and allow unfolding of −1 PRF mRNA structure motifs held at the ribosome's entry site.[13,106] Irrespective of such concerns, unfolding of isolated molecules may still provide clues toward a −1 PRF mechanism in specific cases. For example, in the case of the BWYV pseudoknot, combining unfolding with optical tweezers and computationally by

steered molecular dynamics simulations, identified detailed molecular rearrangements that may explain how the C8U and C8A mutations abolish −1 PRF.[97]

4.2 Elastic Properties of the Single-Stranded RNA Spacer Sequence

Connecting the slippery sequence at the coding site and the downstream mRNA structure motif is a short (~5–6 nucleotides) single-stranded spacer sequence. How rapidly tension builds up upon ribosome motion or is relieved upon mRNA unfolding, depends upon the spacer's elastic properties. Due to lack of any other data, quantitative models usually apply elastic properties as derived from single-molecule stretching experiments using long, spatially unconfined RNA molecules, often homopolymeric to avoid any base pairing.[107–109]

Both AFM and optical tweezers have been used for such single-molecule stretching experiments, which allowed the molecule to be modeled as a so-called worm-like chain model for polymer elasticity, yielding a persistence length, that is, a measure for its stiffness expressed as the typical distance over which a thermal energy unit of k_BT is able to bend the molecule, of approximately 1–1.5 nm, about 30–50 times smaller than for dsDNA. The worm-like chain's force–extension relation then allows computation of the developed tension[53]:

$$F(x) = \frac{k_B T}{L_p}\left[\frac{1}{4(1 - x/L + F/S)^2} - \frac{1}{4} + \frac{x}{L} - \frac{F}{S}\right],$$

with k_B the Boltzmann constant, L_p the persistence length, L the contour length of the molecule, and S the stretching modulus. Examples of force-extension data for homopolymeric single-stranded RNA are shown in Fig. 7.

However, it is not obvious that such data and associated polymer elasticity models are applicable to the short, heteropolymeric and spatially confined spacer sequence. Further complications arise when considering that the spacer is likely to interact with ribosomal RNA and proteins lining the tunnel,[11,110] something not readily captured by any polymer model. In a stochastic model of −1 PRF, Bailey et al. found it necessary to account for the effects of confinement,[24] which proved somewhat problematic as theories either address very strong (channels much narrower than a persistence length) or weak (channels much wider than a persistence length) confinement.[111,112] Recent work such as by Tree et al. explores the intermediate

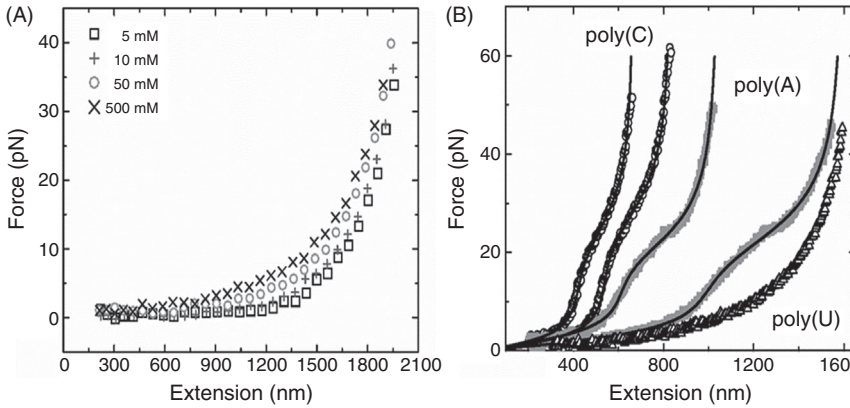

Figure 7 Elasticity of RNA homopolymers. (A) Force-extension of a single poly(U) RNA molecule at varying Na^+ concentrations. A worm-like chain model fits the 500 mM data well but fails to capture the increasingly prevalent electrostatic interactions at low Na^+ concentrations.[107] (B) Unlike poly(U) the force-extension data for poly(A) and poly(C) displays a shoulder indicative of an helix-coil transition. Solid lines fit to a theoretical model.[109] *Reprinted with permission from Seol et al.[107,109] Copyright 2004, 2007 American Physical Society.*

regime of confinement of more direct relevance to the spacer sequence.[113] However, such work often does not address the force–extension relation under moderately confined conditions[114] which would be beneficial for modeling and a quantitative understanding of –1 PRF.[24]

4.3 Probing the Coding Site

What remains is a physical characterization of codon–anticodon interactions, ideally with slippery as well as nonslippery mRNA sequences at the ribosome coding site.

Early work by Uemura et al. report rupture forces for mRNA and prokaryotic ribosomes of 12–15 pN in the absence of a flanking Shine–Dalgarno sequence, but with the A and P sites occupied with tRNAs.[115] Addition of an upstream Shine–Dalgarno sequence stabilizes the mRNA–ribosome complex yielding rupture forces as high as ~27 pN. Vanzi et al. reported sudden slippage of ribosomes on a poly(U) template at typical forces of 10–15 pN.[108] However, active translocation was not demonstrated in these studies. At conditions favorable for active translocation, Skinner[15] found gradual slippage on poly(U) at forces as low as 7–9 pN. These measurements may serve to provide typical baseline force values to be kept in mind in the context of frameshifting.

Recent experiments by the Bustamante and Tinoco groups address translation by active prokaryotic ribosomes at the single-molecule level,[13,14,106,116] but do not yet synthesize a complete answer of how force affects the codon–anticodon interaction and its dynamics on the ribosome during frameshifting. But, since these experimental assays together appear to hold all the ingredients to successfully address this question the experimental geometry and some of their results are outlined later in the chapter. An ingenious single-molecule experiment by Yan et al. primarily probes the effect of the slippery sequence and flanking mRNA structure motifs on codon–anticodon interaction and −1 frameshift efficiency[106] (Fig. 8), whereas Liu et al. explicitly explore the role of force upon translation velocities on nonslippery mRNA sequences.[13]

In Yan's setup the mRNA being translated, containing the frameshift signal is designed as a hairpin sandwiched between two DNA handles with their ends held in optical tweezers and on the tip of a micropipette, respectively (Fig. 8). When during translation, ribosomes move along and unwind the double-stranded hairpin, upon each translated codon six nucleotides

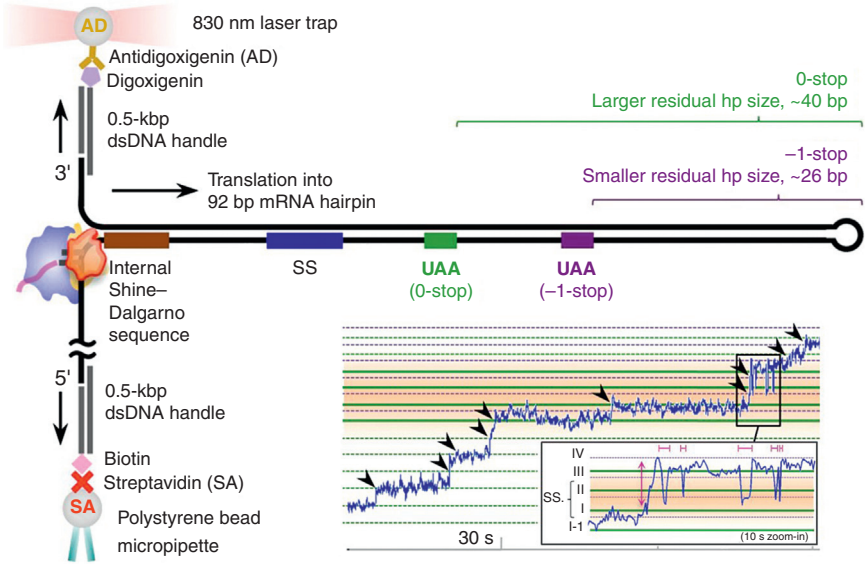

Figure 8 Single-molecule assay for detecting codon-sampling (fluctuations) and −1 frameshifting by individual ribosomes at the slippery sequence (SS). Dotted lines are spaced one codon apart. *Reprinted with permission from Yan et al.*[106] *Copyright 2015 Elsevier.*

become exposed yielding a readily detectable stepwise increase in extension of the trapped DNA–RNA construct. Downstream of the frameshift signal the mRNA contains two spatially well-separated stop codons positioned in the 0 frame and −1 frame, respectively, which serve as frameshift reporters (Fig. 8). Once a ribosome has stalled at one of the stop codons, a long (~40 bp) or short (~26 bp) hairpin remains depending upon the reading frame. The size of the remaining hairpin is readily determined by unfolding using the optical tweezers in force-ramp mode and careful analysis of the increase in extension. The frameshift signal investigated was derived from the *E. coli DnaX* gene and contains three essential RNA elements: a slippery sequence (AAAAAAC) and a downstream RNA structure (a 11 base pair hairpin), two elements also commonly required in viral −1 PRF signals, and in addition a Shine–Dalgarno sequence 10 nucleotides upstream of the slippery sequence. In the assay the *DnaX* hairpin has been extended to contain the frameshift reporters, that is, the two stop codons and hairpin structure.

Using this assay the authors observe stepwise (one codon at a time) unidirectional movement of individual ribosomes along mRNA. However, upon reaching the particular sequence—slippery or not—flanked by the Shine–Dalgarno sequence and the downstream hairpin junction, dynamic (~2 Hz), large scale (~1 codon) back-and-forth fluctuations were observed (Fig. 8). These fluctuations are thought to allow the ribosome to sample the different reading frames (codon sampling). Interestingly, smaller but higher-frequency fluctuations at, for example, 85 Hz as identified by power spectral analysis occur exclusively on the flanked slippery sequence (wild-type and A5G mutant) possibly reflecting ribosome subunit head rotation enhanced by the flanking structural elements. By combining mass spectrometry analysis of translated product and single-molecule translation trajectories the authors identify a wide range of frameshifting pathways, and also find evidence for fidelity checking of codon–anticodon that gives rise to early termination after frameshifting.

In Yan's single-molecule frameshift assay the ribosome has not been conjugated to any surface or microsphere and is free to move along the mRNA threaded through it. This renders it less well suited for probing the force dependence of the observed phenomena, such as the codon sampling, the low- and high-frequency fluctuations, and frameshift efficiency. In the current configuration the entire mRNA–DNA handle complex was held at a constant force of ~18 pN. As the mRNA path through the ribosome is not straight, any tension trying to straighten the mRNA may in principle

reduce accessible mRNA conformations required at the coding site and indirectly destabilize any tRNA–mRNA interactions. However, such concerns appear unwarranted as previous work did not find any tension dependence of translocation step times.[116] In fact, high tension proved beneficial as it rescued long ribosomal stalls, presumably by assisting in unfolding any downstream mRNA roadblocks.

To more directly probe the effect of force at the coding site, the ribosome itself needs to be immobilized, while force pulls on the mRNA.[13,15,108,115] Liu et al. have used such an experimental geometry and measured a single-exponential force dependence of the translational velocity. Surface attachment was via ribosomal protein S16, at point thought to minimally affect ribosome function so that force exerted by the mRNA would predominantly affect the mechanical translocation of the tRNAs from the A and P sites to the P and E site, respectively. A stall force of 13 ± 2 pN was found (by extrapolation), lower than, for example, the unfolding force of stemloop 1 of the BWYV pseudoknot which promotes frameshifting efficiently in prokaryotic translation system.[97,105] This goes to show that downstream mRNA structure motifs can readily regulate translation velocities and therefore may affect associated phenomena such as frameshifting. Also, since the actual applied force did not appear to exceed 10 pN, no mRNA–ribosome ruptures were reported.[108,115]

It should be clear that these assays are uniquely qualified to combine the direct force measurements à la Liu[13] with the reading frameshift reporting mRNA template developed by Yan et al.[106] If then also the mRNA template contains a slippery sequence associated with a mechanically (ie, by force) well-characterized −1 PRF-promoting hairpin or pseudoknot, a complete physical picture of −1 PRF may successfully emerge.

It is noted that while −1 PRF is mainly a eukaryotic phenomenon, all single-molecule translation assays employ prokaryotic ribosomes. However, it has also been shown that −1 PRF systems can frameshift efficiently in prokaryotic translation assays. Furthermore while the biological details may differ, it is not unlikely that the underlying physical principles remain the same.[105,110]

5. CONCLUSIONS

Ever-advancing physical methods and single-molecule assay designs combined with sophisticated data-analysis methods bring a precise physical

mechanism and model of −1 PRF within reach. Although mechanical force has a dominant role to play, the merging picture will likely be rather more complex than any assumed simple correlation of −1 PRF efficiency and RNA pseudoknot unfolding force. How force controls the kinetics of codon sampling at the slippery sequence and of the melting of the downstream mRNA structure is the key to a quantitative model of −1 PRF.

REFERENCES

1. Yu H, Mouw JK, Weaver VM. Forcing form and function: biomechanical regulation of tumor evolution. *Trends Cell Biol.* 2011;21(1):47–56.
2. Diz-Muñoz A, Fletcher DA, Weiner OD. Use the force: membrane tension as an organizer of cell shape and motility. *Trends Cell Biol.* 2013;23(2):47–53.
3. Iskratsch T, Wolfenson H, Sheetz MP. Appreciating force and shape—the rise of mechanotransduction in cell biology. *Nat Rev Mol Cell Biol.* 2014;15(12):825–833.
4. Tinoco I. Force as a useful variable in reactions: unfolding RNA. *Annu Rev Biophys Biomol Struct.* 2004;33:363–385.
5. Roberts AJ, Kon T, Knight PJ, Sutoh K, Burgess SA. Functions and mechanics of dynein motor proteins. *Nat Rev Mol Cell Biol.* 2013;14(11):713–726.
6. Marintchev A. Roles of helicases in translation initiation: a mechanistic view. *Biochim Biophys Acta.* 2013;1829(8):799–809.
7. Qu X, Lancaster L, Noller HF, Bustamante C, Tinoco I. Ribosomal protein S1 unwinds double-stranded RNA in multiple steps. *Proc Natl Acad Sci.* 2012;109(36):14458–14463.
8. Takyar S, Hickerson RP, Noller HF. mRNA helicase activity of the ribosome. *Cell.* 2005;120(1):49–58.
9. von Hippel PH, Delagoutte E. A general model for nucleic acid helicases and their "coupling" within macromolecular machines. *Cell.* 2001;104(2):177–190.
10. Agrawal RK, Heagle AB, Penczek P, Grassucci RA, Frank J. EF-G-dependent GTP hydrolysis induces translocation accompanied by large conformational changes in the 70S ribosome. *Nat Struct Biol.* 1999;6(7):643–647.
11. Yusupova GZ, Yusupov MM, Cate JH, Noller HF. The path of messenger RNA through the ribosome. *Cell.* 2001;106(2):233–241.
12. Wang MD, Schnitzer MJ, Yin H, Landick R, Gelles J, Block SM. Force and velocity measured for single molecules of RNA polymerase. *Science.* 1998;282(5390):902.
13. Liu T, Kaplan A, Alexander L, et al. Direct measurement of the mechanical work during translocation by the ribosome. *eLife.* 2014;3.
14. Qu X, Wen J-D, Lancaster L, Noller HF, Bustamante C, Tinoco I. The ribosome uses two active mechanisms to unwind messenger RNA during translation. *Nature.* 2011;475(7354):118–121.
15. Skinner GM, Seol Y, Visscher K, Dagdug L, Gracía-Colin SL. Translation against an applied force. In: *AIP Conference Proceedings*; 2008:1–10
16. Jacks T, Power MD, Masiarz FR, Luciw PA, Barr PJ, Varmus HE. Characterization of ribosomal frameshifting in HIV-1 gag-pol expression. *Nature.* 1988;331(6153):280–283.
17. Parkin NT, Chamorro M, Varmus HE. Human immunodeficiency virus type 1 gag-pol frameshifting is dependent on downstream mRNA secondary structure: demonstration by expression in vivo. *J Virol.* 1992;66(8):5147–5151.
18. Giedroc DP, Cornish PV. Frameshifting RNA pseudoknots: structure and mechanism. *Virus Res.* 2009;139(2):193–208.
19. Plant EP, Jacobs KLM, Harger JW, et al. The 9-A solution: how mRNA pseudoknots promote efficient programmed −1 ribosomal frameshifting. *RNA.* 2003;9(2):168–174.

20. Plant EP, Dinman JD. Torsional restraint: a new twist on frameshifting pseudoknots. *Nucleic Acids Res.* 2005;33(6):1825–1833.
21. Namy O, Moran SJ, Stuart DI, Gilbert RJC, Brierley I. A mechanical explanation of RNA pseudoknot function in programmed ribosomal frameshifting. *Nature.* 2006;441 (7090):244–247.
22. Brierley I, Jenner AJ, Inglis SC. Mutational analysis of the "slippery-sequence" component of a coronavirus ribosomal frameshifting signal. *J Mol Biol.* 1992;227(2): 463–479.
23. Kim YG, Su L, Maas S, O'Neill A, Rich A. Specific mutations in a viral RNA pseudoknot drastically change ribosomal frameshifting efficiency. *Proc Natl Acad Sci USA.* 1999;96(25):14234–14239.
24. Bailey BL, Visscher K, Watkins J. A stochastic model of translation with −1 programmed ribosomal frameshifting. *Phys Biol.* 2014;11(1):016009.
25. Goldman DH, Kaiser CM, Milin A, Righini M, Tinoco I, Bustamante C. Mechanical force releases nascent chain-mediated ribosome arrest in vitro and in vivo. *Science.* 2015;348(6233):457–460.
26. Mori H, Ito K. The Sec protein-translocation pathway. *Trends Microbiol.* 2001;9 (10):494–500.
27. Hall K, Cole D, Yeh Y, Baskin RJ. Kinesin force generation measured using a centrifuge microscope sperm-gliding motility assay. *BiophysJ.* 1996;71(6):3467–3476.
28. Ashkin A, Dziedzic JM, Bjorkholm JE, Chu S. Observation of a single-beam gradient force optical trap for dielectric particles. *Opt Lett.* 1986;11(5):288.
29. Strick TR, Allemand J-F, Bensimon D, Bensimon A, Croquette V. The elasticity of a single supercoiled DNA molecule. *Science.* 1996;271(5257):1835–1837.
30. Gosse C, Croquette V. Magnetic tweezers: micromanipulation and force measurement at the molecular level. *BiophysJ.* 2002;82(6):3314–3329.
31. De Vlaminck I, Dekker C. Recent advances in magnetic tweezers. *Annu Rev Biophys.* 2012;41(1):453–472.
32. Binnig G, Quate CF, Gerber C. Atomic force microscope. *Phys Rev Lett.* 1986;56 (9):930–933.
33. Rief M. Reversible unfolding of individual titin immunoglobulin domains by AFM. *Science.* 1997;276(5315):1109–1112.
34. Block SM, Goldstein LSB, Schnapp BJ. Bead movement by single kinesin molecules studied with optical tweezers. *Nature.* 1990;348(6299):348–352.
35. Svoboda K, Schmidt CF, Schnapp BJ, Block SM. Direct observation of kinesin stepping by optical trapping interferometry. *Nature.* 1993;365(6448):721–727.
36. Smith S, Finzi L, Bustamante C. Direct mechanical measurements of the elasticity of single DNA molecules by using magnetic beads. *Science.* 1992;258(5085):1122–1126.
37. Visscher K, Schnitzer MJ, Block SM. Single kinesin molecules studied with a molecular force clamp. *Nature.* 1999;400(6740):184–189.
38. Bustamante C, Smith SB, Liphardt J, Smith D. Single-molecule studies of DNA mechanics. *Curr Opin Struct Biol.* 2000;10(3):279–285.
39. Lipfert J, Skinner GM, Keegstra JM, et al. Double-stranded RNA under force and torque: similarities to and striking differences from double-stranded DNA. *Proc Natl Acad Sci USA.* 2014;111(43):15408–15413.
40. Chen H, Yuan G, Winardhi RS, et al. Dynamics of equilibrium folding and unfolding transitions of titin immunoglobulin domain under constant forces. *J Am Chem Soc.* 2015;137(10):3540–3546.
41. Bechtluft P, van Leeuwen RGH, Tyreman M, et al. Direct observation of chaperone-induced changes in a protein folding pathway. *Science.* 2007;318(5855):1458–1461.
42. Mashaghi A, Kramer G, Lamb DC, Mayer MP, Tans SJ. Chaperone action at the single-molecule level. *Chem Rev.* 2014;114(1):660–676.

43. Li PTX, Bustamante C, Tinoco I. Unusual mechanical stability of a minimal RNA kissing complex. *Proc Natl Acad Sci USA.* 2006;103(43):15847–15852.
44. Li PTX, Tinoco I. Mechanical unfolding of two DIS RNA kissing complexes from HIV-1. *J Mol Biol.* 2009;386(5):1343–1356.
45. Ashkin A. Optical trapping and manipulation of neutral particles using lasers. *Proc Natl Acad Sci USA.* 1997;94(10):4853.
46. Block S, Svoboda K. Biological applications of optical forces. *Annu Rev Biophys Biomol Struct.* 1994;23:247–285.
47. Neuman KC, Block SM. Optical trapping. *Rev Sci Instrum.* 2004;75(9):2787–2809.
48. Visscher K, Block SM. Versatile optical traps with feedback control. *Methods Enzymol.* 1998;298:460–489.
49. Neuman KC, Nagy A. Single-molecule force spectroscopy: optical tweezers, magnetic tweezers and atomic force microscopy. *Nat Methods.* 2008;5(6):491–505.
50. Greenleaf W, Woodside M, Abbondanzieri E, Block S. Passive all-optical force clamp for high-resolution laser trapping. *Phys Rev Lett.* 2005;95(20):208102.
51. Liphardt J, Onoa B, Smith SB, Tinoco Jr I, Bustamante C. Reversible unfolding of single RNA molecules by mechanical force. *Science.* 2001;292(5517):733.
52. Cecconi C. Direct observation of the three-state folding of a single protein molecule. *Science.* 2005;309(5743):2057–2060.
53. Wang MD, Yin H, Landick R, Gelles J, Block SM. Stretching DNA with optical tweezers. *Biophys J.* 1997;72(3):1335–1346.
54. Visscher K, Block SM. Versatile optical traps with feedback control. In: *Methods in Enzymology.* Vol 298. Elsevier; 1998:460–489. http://linkinghub.elsevier.com/retrieve/pii/S0076687998980405
55. Gittes F, Schmidt CF. Interference model for back-focal-plane displacement detection in optical tweezers. *Opt Lett.* 1998;23(1):7.
56. Rohrbach A, Stelzer EHK. Three-dimensional position detection of optically trapped dielectric particles. *J Appl Phys.* 2002;91(8):5474.
57. Perkins TT. Ångström-precision optical traps and applications. *Annu Rev Biophys.* 2014;43(1):279–302.
58. Walder R, Paik DH, Bull MS, Sauer C, Perkins TT. Ultrastable measurement platform: sub-nm drift over hours in 3D at room temperature. *Opt Express.* 2015;23(13):16554–16564.
59. Smith SB, Cui Y, Bustamante C. Overstretching B-DNA: the elastic response of individual double-stranded and single-stranded DNA molecules. *Science.* 1996;271(5250):795–799.
60. Abbondanzieri EA, Greenleaf WJ, Shaevitz JW, Landick R, Block SM. Direct observation of base-pair stepping by RNA polymerase. *Nature.* 2005;438(7067):460–465.
61. Moffitt JR, Chemla YR, Izhaky D, Bustamante C. Differential detection of dual traps improves the spatial resolution of optical tweezers. *Proc Natl Acad Sci USA.* 2006;103(24):9006–9011.
62. Elms PJ, Chodera JD, Bustamante CJ, Marqusee S. Limitations of constant-force-feedback experiments. *Biophys J.* 2012;103(7):1490–1499.
63. Phillips DB, Padgett MJ, Hanna S, et al. Shape-induced force fields in optical trapping. *Nat Photon.* 2014;8(5):400–405.
64. Woodside MT, Anthony PC, Behnke-Parks WM, Larizadeh K, Herschlag D, Block SM. Direct measurement of the full, sequence-dependent folding landscape of a nucleic acid. *Science.* 2006;314(5801):1001–1004.
65. Ribezzi-Crivellari M, Huguet JM, Ritort F. Counter-propagating dual-trap optical tweezers based on linear momentum conservation. *Rev Sci Instrum.* 2013;84(4):043104.
66. Ribezzi-Crivellari M, Ritort F. Free-energy inference from partial work measurements in small systems. *Proc Natl Acad Sci USA.* 2014;111(33):E3386–E3394.

67. de Messieres M, Brawn-Cinani B, La Porta A. Measuring the folding landscape of a harmonically constrained biopolymer. *BiophysJ.* 2011;100(11):2736–2744.
68. Dulin D, Vilfan ID, Berghuis BA, et al. Elongation-competent pauses govern the fidelity of a viral RNA-dependent RNA polymerase. *Cell Rep.* 2015;10(6):983–992.
69. Halvorsen K, Wong WP. Massively parallel single-molecule manipulation using centrifugal force. *BiophysJ.* 2010;98(11):L53–L55.
70. Cumpson PJ, Clifford CA, Portoles JF, Johnstone JE, Munz M. Cantilever spring-constant calibration in atomic force microscopy. In: Bhushan B, Fuchs H, Tomitori M, eds. In: *Applied Scanning Probe Methods VIII. Berlin, Heidelberg: Springer Berlin Heidelberg;2008:. http://link.springer.com/10.1007/978-3-540-74080-3_8*
71. Churnside AB, Perkins TT. Ultrastable atomic force microscopy: improved force and positional stability. *FEBS Lett.* 2014;588(19):3621–3630.
72. Li L, Wetzel S, Plückthun A, Fernandez JM. Stepwise unfolding of ankyrin repeats in a single protein revealed by atomic force microscopy. *BiophysJ.* 2006;90(4):L30–L32.
73. Zhmurov A, Dima RI, Barsegov V. Order statistics theory of unfolding of multimeric proteins. *BiophysJ.* 2010;99(6):1959–1968.
74. Harlepp S, Marchal T, Robert J, et al. Probing complex RNA structures by mechanical force. *Eur Phys J E Soft Matter.* 2003;12(4):605–615.
75. Akeson M, Branton D, Kasianowicz JJ, Brandin E, Deamer DW. Microsecond time-scale discrimination among polycytidylic acid, polyadenylic acid, and polyuridylic acid as homopolymers or as segments within single RNA molecules. *Biophys J.* 1999;77 (6):3227–3233.
76. Meller A, Nivon L, Brandin E, Golovchenko J, Branton D. Rapid nanopore discrimination between single polynucleotide molecules. *Proc Natl Acad Sci USA.* 2000;97 (3):1079–1084.
77. Li J, Stein D, McMullan C, Branton D, Aziz MJ, Golovchenko JA. Ion-beam sculpting at nanometre length scales. *Nature.* 2001;412(6843):166–169.
78. Storm AJ, Chen JH, Ling XS, Zandbergen HW, Dekker C. Fabrication of solid-state nanopores with single-nanometre precision. *Nat Mater.* 2003;2(8):537–540.
79. Li J, Gershow M, Stein D, Brandin E, Golovchenko JA. DNA molecules and configurations in a solid-state nanopore microscope. *Nat Mater.* 2003;2(9):611–615.
80. Dudko OK, Mathé J, Szabo A, Meller A, Hummer G. Extracting kinetics from single-molecule force spectroscopy: nanopore unzipping of DNA hairpins. *BiophysJ.* 2007;92 (12):4188–4195.
81. van den Hout M, Vilfan ID, Hage S, Dekker NH. Direct force measurements on double-stranded RNA in solid-state nanopores. *Nano Lett.* 2010;10(2):701–707.
82. Dekker C. Solid-state nanopores. *Nat Nanotechnol.* 2007;2(4):209–215.
83. Tinoco I, Li PTX, Bustamante C. Determination of thermodynamics and kinetics of RNA reactions by force. *Q Rev Biophys.* 2006;39(04):325.
84. Wen J-D, Manosas M, Li PTX, et al. Force unfolding kinetics of RNA using optical tweezers. I. Effects of experimental variables on measured results. *Biophys J.* 2007;92 (9):2996–3009.
85. Manosas M, Wen J-D, Li PTX, et al. Force unfolding kinetics of RNA using optical tweezers. II. Modeling experiments. *BiophysJ.* 2007;92(9):3010–3021.
86. Jarzynski C. Nonequilibrium equality for free energy differences. *Phys Rev Lett.* 1997;78 (14):2690–2693.
87. Crooks GE. Entropy production fluctuation theorem and the nonequilibrium work relation for free energy differences. *Phys Rev E.* 1999;60(3):2721–2726.
88. Liphardt J, Dumont S, Smith SB, Tinoco I, Bustamante C. Equilibrium information from nonequilibrium measurements in an experimental test of Jarzynski's equality. *Science.* 2002;296(5574):1832–1835.

89. Collin D, Ritort F, Jarzynski C, Smith SB, Tinoco I, Bustamante C. Verification of the Crooks fluctuation theorem and recovery of RNA folding free energies. *Nature.* 2005;437(7056):231–234.
90. Woodside MT, Block SM. Reconstructing folding energy landscapes by single-molecule force spectroscopy. *Annu Rev Biophys.* 2014;43(1):19–39.
91. Bryngelson JD, Onuchic JN, Socci ND, Wolynes PG. Funnels, pathways, and the energy landscape of protein folding: a synthesis. *Proteins Struct Funct Genet.* 1995;21 (3):167–195.
92. Dudko OK, Graham TGW, Best RB. Locating the barrier for folding of single molecules under an external force. *Phys Rev Lett.* 2011;107(20):208301.
93. Du R, Pande VS, Grosberg AY, Tanaka T, Shakhnovich ES. On the transition coordinate for protein folding. *J Chem Phys.* 1998;108(1):334.
94. Chodera JD, Pande VS. Splitting probabilities as a test of reaction coordinate choice in single-molecule experiments. *Phys Rev Lett.* 2011;107(9):098102.
95. Neupane K, Manuel AP, Lambert J, Woodside MT. Transition-path probability as a test of reaction-coordinate quality reveals DNA hairpin folding is a one-dimensional diffusive process. *J Phys Chem Lett.* 2015;6(6):1005–1010.
96. Onoa B. Identifying kinetic barriers to mechanical unfolding of the *T. thermophila* ribozyme. *Science.* 2003;299(5614):1892–1895.
97. White KH, Orzechowski M, Fourmy D, Visscher K. Mechanical unfolding of the beet Western yellow virus −1 frameshift signal. *J Am Chem Soc.* 2011;133(25):9775–9782.
98. Hansen TM, Reihani SNS, Oddershede LB, Sørensen MA. Correlation between mechanical strength of messenger RNA pseudoknots and ribosomal frameshifting. *Proc Natl Acad Sci USA.* 2007;104(14):5830–5835.
99. Chen G, Chang K-Y, Chou M-Y, Bustamante C, Tinoco I. Triplex structures in an RNA pseudoknot enhance mechanical stability and increase efficiency of −1 ribosomal frameshifting. *Proc Natl Acad Sci USA.* 2009;106(31):12706–12711.
100. Green L, Kim C-H, Bustamante C, Tinoco I. Characterization of the mechanical unfolding of RNA pseudoknots. *J Mol Biol.* 2008;375(2):511–528.
101. Ritchie DB, Foster DAN, Woodside MT. Programmed −1 frameshifting efficiency correlates with RNA pseudoknot conformational plasticity, not resistance to mechanical unfolding. *Proc Natl Acad Sci USA.* 2012;109(40):16167–16172.
102. Ritchie DB, Soong J, Sikkema WKA, Woodside MT. Anti-frameshifting ligand reduces the conformational plasticity of the sars virus pseudoknot. *J Am Chem Soc.* 2014;136 (6):2196–2199.
103. de Messieres M, Chang J-C, Belew AT, Meskauskas A, Dinman JD, La Porta A. Single-molecule measurements of the CCR5 mRNA unfolding pathways. *BiophysJ.* 2014;106 (1):244–252.
104. Mazauric M-H, Seol Y, Yoshizawa S, Visscher K, Fourmy D. Interaction of the HIV-1 frameshift signal with the ribosome. *Nucleic Acids Res.* 2009;37(22):7654–7664.
105. Mazauric M-H, Leroy J-L, Visscher K, Yoshizawa S, Fourmy D. Footprinting analysis of BWYV pseudoknot-ribosome complexes. *RNA.* 2009;15(9):1775–1786.
106. Yan S, Wen J-D, Bustamante C, Tinoco I. Ribosome excursions during mRNA translocation mediate broad branching of frameshift pathways. *Cell.* 2015;160(5):870–881.
107. Seol Y, Skinner G, Visscher K. Elastic properties of a single-stranded charged homopolymeric ribonucleotide. *Phys Rev Lett.* 2004;93(11):118102.
108. Vanzi F, Takagi Y, Shuman H, Cooperman BS, Goldman YE. Mechanical studies of single ribosome/mRNA complexes. *BiophysJ.* 2005;89(3):1909–1919.
109. Seol Y, Skinner GM, Visscher K, Buhot A, Halperin A. Stretching of homopolymeric RNA reveals single-stranded helices and base-stacking. *Phys Rev Lett.* 2007;98(15): 158103.

110. Pisarev AV, Kolupaeva VG, Yusupov MM, Hellen CU, Pestova TV. Ribosomal position and contacts of mRNA in eukaryotic translation initiation complexes. *EMBO J.* 2008;27(11):1609–1621.
111. Brochard F, de Gennes PG. Dynamics of confined polymer chains. *J Chem Phys.* 1977;67 (1):52.
112. Odijk T. The statistics and dynamics of confined or entangled stiff polymers. *Macromolecules.* 1983;16(8):1340–1344.
113. Tree DR, Wang Y, Dorfman KD. Mobility of a semiflexible chain confined in a nanochannel. *Phys Rev Lett.* 2012;108(22):228105.
114. Wang J, Gao H. Stretching a stiff polymer in a tube. *J Mater Sci.* 2007;42(21):8838–8843.
115. Uemura S, Dorywalska M, Lee T-H, Kim HD, Puglisi JD, Chu S. Peptide bond formation destabilizes Shine–Dalgarno interaction on the ribosome. *Nature.* 2007;446(7134):454–457.
116. Wen J-D, Lancaster L, Hodges C, et al. Following translation by single ribosomes one codon at a time. *Nature.* 2008;452(7187):598–603.